A classroom jumping ring

Carl S. Schneider and John P. Ertel
Physics Department, U.S. Naval Academy, Annapolis, Maryland 21402

(Received 24 February 1997; accepted 29 January 1998)

We present the design of a compact alternating current jumping ring apparatus which can electromagnetically launch conducting rings across a classroom. Jump energy and height are calculated for core and thin ring length, radius, thickness, and material. The effects of core saturation, permeability, hysteresis and demagnetizing field, ring shielding, and convective derivative are described. Rings with even small phase lag can pass by the magnetic pole of the primary in one-quarter of a cycle. Large ring size relative to skin depth delays the ring current close to the 180 deg of Lenz's law. Contactless jump height measurement enables ring resistivity determination. Demonstrating the effects of voltage, frequency, conductivity, permeability, and geometry contributes to understanding electromagnetism in the classroom.

I. INTRODUCTION

Elihu Thomson was 34 years old in May of 1887 as he presented to the American Institute of Electrical Engineers in New York a copper ring jumping due to electromagnetic repulsion. The battle in the market between his ac dynamos and the dc system of Edison had grown for a decade, and each sought a final demonstration of its supremacy. Direct current supporters electrocuted dogs with ac current to mislead the public into unfounded fears, while Thomson explained the need to transform voltages in a national electrical network, eliminating dangerous and unsightly backyard power plants. The jumping ring forcefully showed the potential of the induction motor, and the battle was won. The succeeding merger with Edison and his light bulb lead to the formation of the General Electric Company in 1892, and the beginning of the electrical age.[1]

The jumping ring has since symbolized Faraday's and Lenz's laws, and the demonstration has been used by many teachers. In his 1938 ''Demonstration Experiments in Physics'' Sutton[2] described a broad flat ring jumping from the top of the primary. In his ''Lectures on Physics'' in 1964, Feynman[3] used a flat ring, and described the magnetic poles of the primary and jumping ring which repel each other. In AAPT's ''Physics Demonstration Experiments'' by Meiners[4] in 1970, a flat aluminum pan was suspended above an ac magnet. Mak and Young[5] in 1986 floated a thin ring, calculating the average force of levitation from the induced voltage, resistance, frequency, and phase shift. The ''Video Encyclopedia of Physics Demonstrations'' [6] in 1992 used a flat ring commenting that the explanation was ''complex.'' Jonathon Hall[7] in 1997 calculated the frequency dependence of the force on a suspended ring. The jumping ring apparatus used in many lecture halls has been massive, weighing several hundred pounds and taking great effort to build. In this paper we design a compact optimized ac apparatus and determine analytically and by numerical integration the velocity, energy, and jump height of a conducting ring repelled from the magnetic core.

II. THE PRIMARY CIRCUIT

This classroom apparatus, shown in Fig. 1, is made of an 8 in. length of $\frac{1}{2}$ in. i.d. iron gas pipe wound with two 400-turn layers of 0.38-mm-diam copper wire, across 120 V rms 60-Hz source. As shown in Fig. 2, the pipe is slit and the pipe core is filled with rods, cut from coat hangers, 2 in. longer than the pipe to allow removal in demonstrating resistive and inductive impedance. This core design nearly removes eddy current losses in the primary, which would be substantial since the skin depth, t_s, of iron of permeability, μ, induction, B, and conductivity, σ, in a magnetic field, H, of angular frequency, ω, is[8]

$$t_s=(2/\omega\mu\sigma)^{1/2}=(2H/\omega B\sigma)^{1/2} \tag{1}$$

or about 5 mm for our system. When the primary is excited by a 60-Hz voltage source, magnetic flux, $\Phi_0 \sin \omega t$, passes through the primary turns. Faraday's law describes the voltage, V, induced around any closed path in the primary or the ring:

$$V=-d\Phi/dt=-\omega\Phi_0 \cos \omega t. \tag{2}$$

Constant permeability is necessary to maintain the sinusoidal waveform, and is a good approximation for our core shape since the demagnetization field of the magnetic poles, described in more detail below, far exceeds the coercive field of the iron, and hysteresis is small. For both the primary and the secondary, the current, I, is limited by the resistance, R, around the path and the self-inductance, L, through Kirchhoff's law:

$$V=IR+L\ dI/dt=IZ, \tag{3}$$

where for harmonic functions $Z=R+i\omega L$ is the complex sum of the resistive and reactive impedance. The resistance and inductive reactance components are 90° out of phase, or orthogonal in the complex plane as shown in Fig. 3, causing the current to lag behind the voltage by the phase shift, ϕ. Saturated ferromagnetic induction, B_s, in the iron core enhances energy density. Iron requires a magnetic field to overcome its coercive field, the demagnetizing field of the pipe ends, and its crystalline anisotropy, rotating the magnetization toward the solenoid axis. The voltage necessary to saturate the iron is the back electromotive force (emf) induced in the primary plus that to produce the phase shifted current and magnetic field above. Dividing Eq. (3) by the induced voltage at saturation, V_N, the magnetic induction becomes scaled to its saturation value and the magnetic field is scaled by the field, H_R, which the induced voltage would

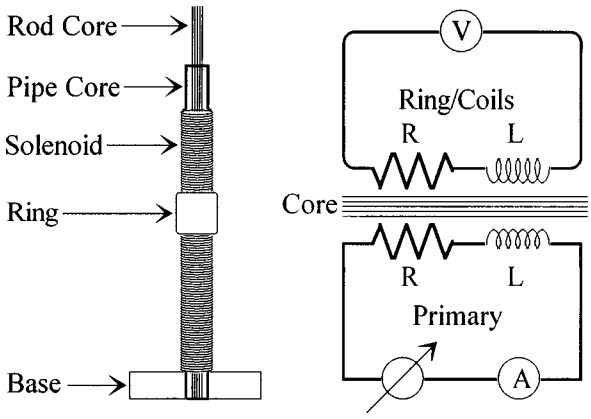

Fig. 1. The jumping ring primary is made of 8 in. of $\frac{1}{2}$ in. i.d. slotted iron gas pipe wound with two 400-turn layers of 0.38-mm-diam copper wire across 120 V rms 60-Hz source and filled with iron rods.

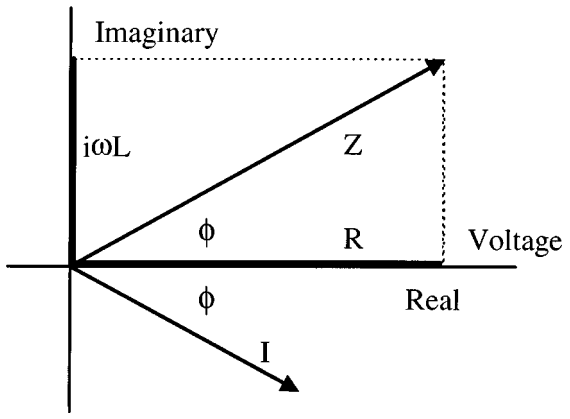

Fig. 3. The primary core and conducting ring have complex impedance for sinusoidal voltage, causing the current to lag the induced voltage in phase.

produce across the resistance of the primary turns, N, over length, l:

$$V/V_N = iB/B_s + H/H_R,$$

where

$$V_N = NAB_s\omega, \quad H_R = NV_N/lR. \tag{4}$$

Choosing N to be 800, B/B_s and H/H_R are both near unity and $V/V_N = \sqrt{2}$ at a 170 V peak. The 800 turns yield $H_R = 60$ kA/m, while using 1200 turns would reduce the jump height and primary heating, as would thinner wire. The magnetic induction has contributions from the magnetic field and the induced magnetization density, M:

$$B = \mu_0(H+M), \quad \text{where} \quad M_s/M = 1 + H_{sc}/H \tag{5}$$

adequately models the approach to saturation. The scaling magnetic field, H_{sc} is initially DM_s, where the demagnetization factor, D, is by Gauss's law roughly the solid angle that the poles subtend at the core center, which is about 0.003 for the pipe plus 0.001 for the long rods.[9] The saturation magnetization is $M_s = 1700$ kA/m and the demagnetizing field of the pipe is 7 kA/m, about ten times the coercive field of mild steel. At larger fields, H_{sc} becomes the 40-kA/m crystalline anisotropy field which rotates the domains of iron. As shown in Fig. 4, the initial slope is nearly unity, decreasing as the core saturates to a final slope of $H_R/M_s = 0.035$ due to the field of the coil. The magnetic induction, B, was determined for many input voltages by integrating over time the measured voltage of a ten-turn search coil at the middle of the core. The flux for 120 V, 435 μWb, equals the core area 191 μm^2 multiplied by magnetic induction, 2.28 T. When the rods are removed from the pipe, the primary impedance of 11 Ω decreases essentially to its resistance of 8 Ω. The 15-A current generates about 1800 W of resistive heating in the primary, so the current for launch is enabled using a momentary switch and the primary is protected with a 3-A fuse. The inductive reactance of the primary is 8 Ω; its inductance is 21 mH and its average relative permeability is about 30, less than $1/D$ and the material permeability as expected.[10] The primary, covered with clear varnish for safety and visibility, can provide a 50-mm-long ring about 1 J in a cycle. The efficiency of coupling can be quite high for large rings when eddy currents in the primary are prevented.

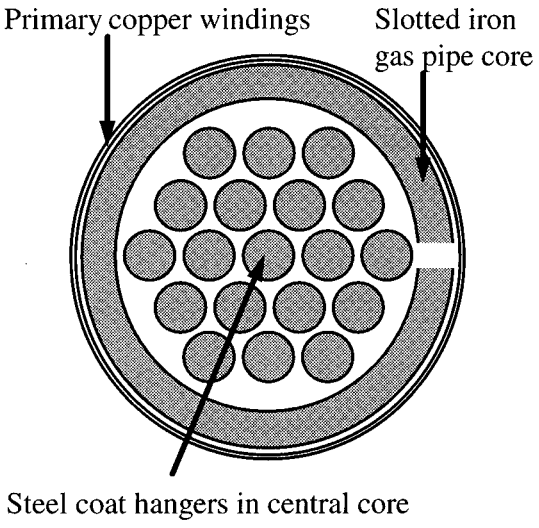

Fig. 2. A top view of the jumping ring apparatus shows the slotted iron gas pipe and the individual rods cut from coat hangers to reduce eddy currents.

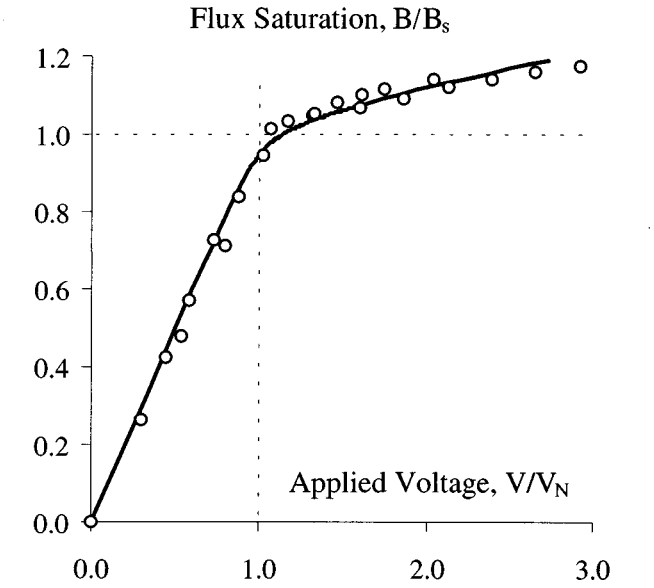

Fig. 4. Voltage causes ferromagnetic core saturation and then heats the copper turns in the primary.

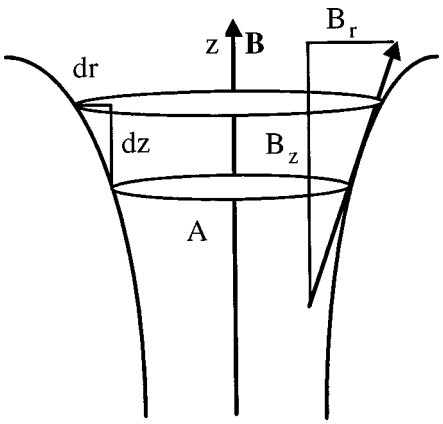

Fig. 5. The radial B field arises from the divergence of the B field in the primary.

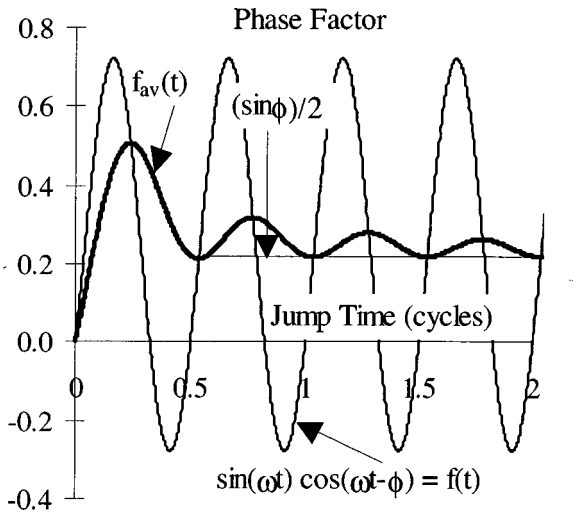

Fig. 6. The average of $\sin \omega t \cos(\omega t-\phi)$ exceeds $(\sin \phi)/2$ for fast jumps.

III. THE RING CIRCUIT

The current in the ring, I_2, experiences a Lorentz force in the magnetic field, B, of the primary:

$$\mathbf{F}=\oint_{\text{ring}} d\mathbf{l}\mathbf{I}_2\times\mathbf{B}=2\pi r I_2 B_r \hat{k}, \tag{6}$$

where $\hat{k}$ is along the vertical axis of the core. Since the current in the ring is azimuthal, vertical forces arise from radial or fringing components of the B field. The radial component, B_r, is related to the axial component, B_z, by conservation of flux, or Gauss's law, as shown in Fig. 5:

$$d\Phi=B_r 2\pi r dz+\pi r^2 dB_z=0, \quad B_r=-(r/2)dB_z/dz. \tag{7}$$

The magnetic flux enters the cylinder axially from the bottom through area A_1 and some is lost radially through its sides. The vertical force on the ring of impedance Z_2 is then

$$F_z=-A_2 I_2 dB_z/dz=-A_2 dB_z/dz(V_2/Z_2)$$
$$=-A_2 dB_z/dz(\omega A_1 B_z/Z_2), \tag{8}$$

which is the axial force on the ring's magnetic dipole moment, $A_2 I_2$, in the axial magnetic field gradient. The ring is repelled from the maximum magnetic induction and the force increases from zero at the center to a peak near either pole. If the axial B field of the primary varies as $\sin \omega t$, then the ring current varies as its phase shifted time derivative, $\cos(\omega t-\phi)$. Temporal averaging may be performed first, independent of position, over the time interval in which the force is nearly constant, and Eq. (8) is multiplied by the phase factor of Eq. (9), shown in Fig. 6:

$$\int_0^{t_m} \sin \omega t \cos(\omega t-\phi)dt/t_m$$
$$=\sin \phi(1/2-\sin 2\omega t_m/4\omega t_m)+\cos \phi \sin^2 \omega t_m/2\omega t_m, \tag{9}$$

which exceeds $(\sin \phi)/2=\omega L_2/2Z_2$, reaching about 1/2 for both fast jumps at small phase lag and slow jumps for large rings. The flux and its gradient are shown in Figs. 7 and 8. The jump time, t_m, is essentially the time for the ring to pass the magnetic pole of the primary, not the entire length of the solenoid. The work done by this axial force from the release height, z_0, to its maximum height, z_0+h, is then

$$W=\int_{z_0}^{z_0+h} F_z\, dz=(\omega A_1 A_2 B_z^2/2Z_2)(\omega L_2/2Z_2)$$
$$=\omega^2 A_1 A_2 B^2 L_2/4Z_2^2, \tag{10}$$

where Z_2 is now the magnitude of the impedance of the ring and the initial value of B_z near the center is B. When the core is driven to magnetic fields much larger than H_{sc}, saturation occurs earlier in the cycle and the flux varies more like a square wave. The induced current, lagging by as much as 90 deg in phase, can then peak at larger flux and increase the phase factor, as for a direct current step. For sinusoidal flux, the energy of a slow, close thin ring ($A_1=A_2$) can be expressed in terms of its self-inductance and current or voltage:

$$W=mgh=L_2(\omega\Phi/Z_2)^2/2=L_2(V_2/Z_2)^2/2=L_2 I_2^2/2, \tag{11}$$

where flux, Φ, voltage, and current here are root mean square values. The tangent of the phase angle for the secondary impedance can be evaluated in terms of the material size and

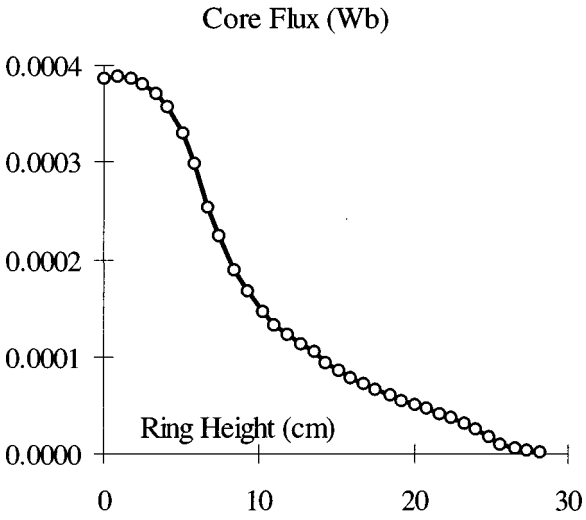

Fig. 7. Integrating the voltage over a positive half cycle gives the magnetic flux of the primary shielded by an aluminum ring, which decreases from a maximum at its center.

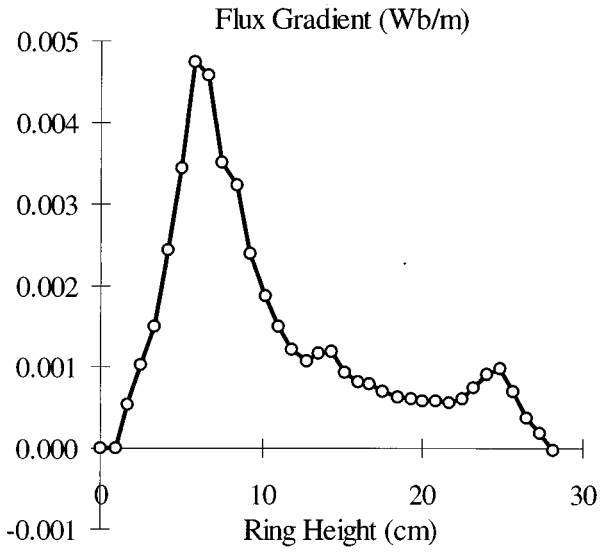

Fig. 8. The gradient of the magnetic flux of the primary shows the poles due to both the pipe and the rods within.

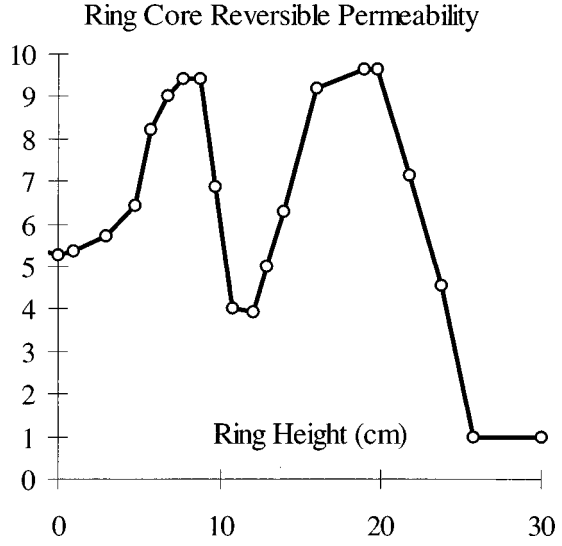

Fig. 10. The relative reversible permeability of the primary measured with a 4-A dc bias current is not homogeneous, but decreased to 1.4 with 13-A dc bias current.

skin depth. This dimensionless size factor for a thin ring of radius, r_2, thickness, t_2, and length, l, is

$$S=\tan\,\phi=\omega L_2/R_2=Kr_2t_2/t_s^2$$

since

$$L_2=\Phi_{22}/I_2=\mu K\pi r_2^2/l,\quad R_2=2\pi r_2/\sigma l t_2. \tag{12}$$

Here Φ_{22} is the flux created and sensed by the ring carrying current I_2 and K is the Nagoaka ratio[11] of this finite solenoid flux to that of one with infinite length, as shown in Fig. 9. The relative permeability, μ, within the ring is not unity since it contains magnetic material, but is rather the reversible value, which was measured using excitation and sense coils moved together along the primary carrying a dc bias current of 4 A. This permeability, shown in Fig. 10, varies with position, and should monotonically decrease from the demagnetized value as magnetization increases to saturation.[12] The lack of monotonic variation suggests that the 4 A bias current did not overcome the inhomogeneous magnetic state in the primary when the current was switched off. At higher dc bias currents of 7 and 13 A, typical during the jump, the relative reversible permeability decreased to 2.1 and 1.4, respectively.

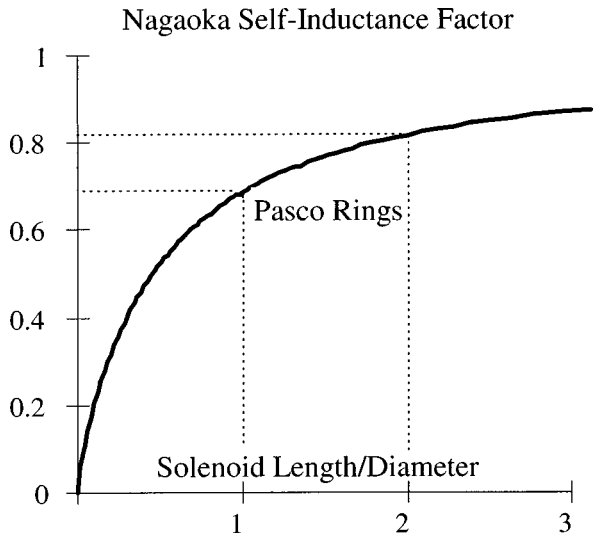

Fig. 9. The self-inductance of a ring is the product of its area per length, permeability, and Nagoaka factor K.

The self-inductance and impedance can now be expressed in terms of the size factor:

$$L_2=R_2S/\omega,\quad Z_2^2=R_2^2(1+S^2). \tag{13}$$

The scaled jump height in terms of phase shift, ϕ, and ring size, S, can now be calculated from Eq. (10) for a thin slow ring of mass, $2\pi r_2t_2l\rho$, where ρ is density, in terms of peak values:

$$\begin{aligned}4mghK\mu A_1/l\Phi_{\rm net}^2&=4mghK\mu/B^2A_1l\\&=\sin^2\,\phi=S^2/(1+S^2),\end{aligned} \tag{14}$$

where the first form is expressed in terms of the net flux from the primary and ring, evidenced by the voltages measured with a sense coil and shown in Fig. 11. The second form shows the jump energy mgh scaled by the energy density $B^2/4\mu$ averaged over both space and time, multiplied by core volume A_1l contained by the ring. The net flux is the primary flux, Φ_1, less the out-of-phase component of the ring flux, Φ_2:

$$\begin{aligned}\Phi_{\rm net}=\Phi_1-\Phi_2\,\sin\,\phi&=\Phi_1-L_2I_2\,\sin\,\phi\\&=\Phi_1/(1+\sin^2\,\phi)\\&=\Phi_1(1+S^2)/(1+2S^2)\end{aligned} \tag{15}$$

since $I_2Z_2=\omega\Phi_{\rm net}$. The net flux decreases from the full primary flux to half for large rings, $S\gg1$. The jump height dependence on ring phase lag, conductivity, and frequency is then

$$\begin{aligned}16mgh(\sigma,\omega)K\mu A_1/\Phi_1^2l&=4\,\sin^2\,\phi/(1+\sin^2\,\phi)^2\\&=4S^2(1+S^2)/(1+2S^2)^2\end{aligned} \tag{16}$$

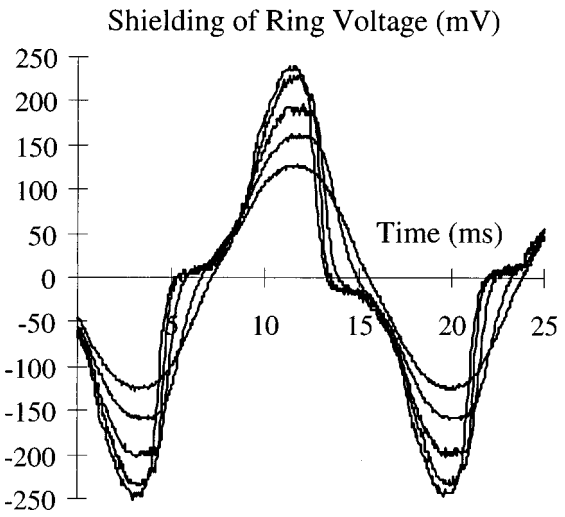

Fig. 11. Shielding of voltages sensed by a coil around the core at launch position increases with the length of aluminum rings around the coil.

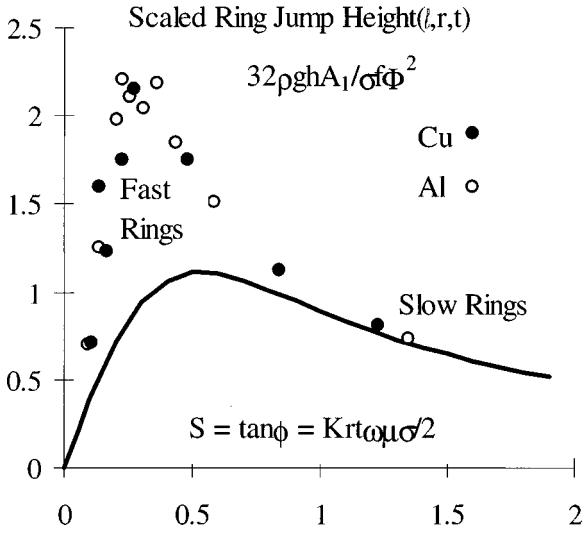

Fig. 13. The time average fraction of the force is (sin ϕ)/2 for slow rings, but it rises rapidly to nearly a constant value of 0.5 at small phase lags as currents saturate and mass increases.

and is plotted in Fig. 12. The maximum jump height at high conductivity is about 6 m for Pasco aluminum tubing, with uncertainty due to initial phase at launch, time averaging, nonsinusoidal flux, Nagoaka constant for thick rings, and air drag. Liquid nitrogen temperature greatly increases conductivity and small cold rings jump much higher than at room temperature. Relative permeability of the primary for aluminum and copper ring samples was found to be 1.6 from Eq. (16) and the data.

The jump height dependence on frequency, f, phase shift, ϕ, and ring length, radius, and thickness, is

$$32\rho gh(l,r,t)A_1/\sigma f\Phi_1^2 = 4\sin\phi\cos\phi/(1+\sin^2\phi)^2 = 4S(1+S^2)/(1+2S^2)^2, \quad (17)$$

which is plotted in Fig. 13. These data confirm that the average force fraction of Eq. (9) exceeds (sin ϕ)/2 as the jump time decreases, until it reaches a nearly constant value of $\frac{1}{2}$. Impurities in the Pasco aluminum were measured to be primarily 1% magnesium using our proton induced X-ray emission (PIXE) system. This is sufficiently low that resistivity is nearly linear with absolute temperature. The conductivity of the Pasco tube was measured using the four probe procedure to be 29 MS/m, below the 35 MS/m of pure aluminum. The conductivity of copper was taken to be the published 59 MS/m. The jump height of large, slow, loosely fitting Pasco aluminum rings at room temperature fit a magnetic flux of 370 μWb. The jump height for the precisely fitting large copper rings fit the full 435-μWb magnetic flux. The maximum jump heights are greater than predicted due to the short time of the force in Fig. 6; the jump occurs essentially in a quarter of a cycle near the magnetic pole of the primary, and this was confirmed by numerical computation as described in the next section. A 50-mm length of aluminum ring can be cut from the 2 m of tubing normally used to show the terminal velocity in gravity of a magnet due to eddy current braking and purchased from the Pasco Company. It has a resistance of 20 $\mu\Omega$, an inductance of 16 nH, a size factor of 0.32, a current of 9-kA peak, an energy, mgh, of 0.82 J, and a jump height of 3.0 m.

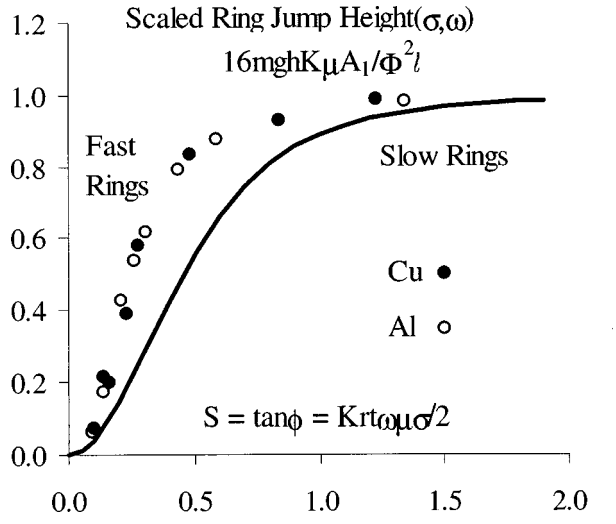

Fig. 12. The ring jump height saturates with conductivity and frequency. Relative permeability for these data was 1.6 for both aluminum and copper.

IV. NUMERICAL COMPUTATION

An alternative to the thin ring sinusoidal theory of ring jump height is numerical integration. We replace the phase lag of Eq. (9) with an iterative form of Eq. (3):

$$I_{n+1} = I_n + (V_{\text{eff}}(z_n,t_n) - I_n R)\Delta t/L. \quad (18)$$

Voltages were measured inside and outside the ring every 40 μs and 7 mm above the middle of the primary, and several of these curves are shown in Fig. 14. The observed peak voltage was less than $V_0/N = 170/800 = 212$ mV due to self-shielding by the ring, which increases with its thickness and its length. Shielding may be seen dramatically by placing a copper or aluminum pipe around the entire apparatus and observing the jump height reduced in proportion to the pipe wall thickness. Not only does the voltage decrease with ring height, but also it is increasingly delayed in time; the ring surfs the waveform as it is launched.

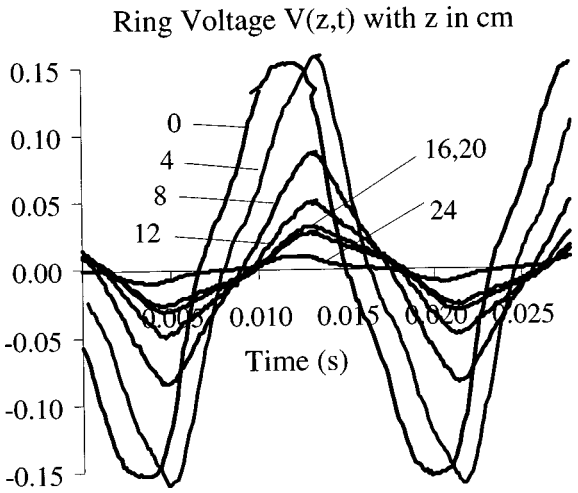

Fig. 14. Sense coils on the conducting ring show decreased voltage and increased time lag with ring height above the middle of the primary.

Faraday's law and the convective derivative quantitatively predict the drag induced from the motion of a conducting ring leaving the magnetic flux:

$$V_{\text{eff}}(z,t) = -d\Phi/dt = -\partial\Phi(z,t)/\partial t - v_z \partial\Phi(z,t)/\partial z. \quad (19)$$

The scale time and distance in which change occurs for these derivatives suggest that the maximum speed of a ring is the product of the scale length and frequency. The corresponding acceleration is the product of the scale length and square of the frequency. For our apparatus, the jump height of every length Pasco aluminum ring cooled with liquid nitrogen was measured to be about 6.4 m, and a maximum independent of ring length was reached.

The force on the ring at any time during the integration is

$$F_n = ma_n = I_n (r_2/r_1)^2 \Delta\Phi_n(z_n, t_n)/\Delta z \quad (20)$$

from which the speed and height can be determined by direct summation over time steps, Δt. The results for a ring launched near maximum flux (the primary center) and near maximum gradient (the primary poles) are shown in Fig. 15.

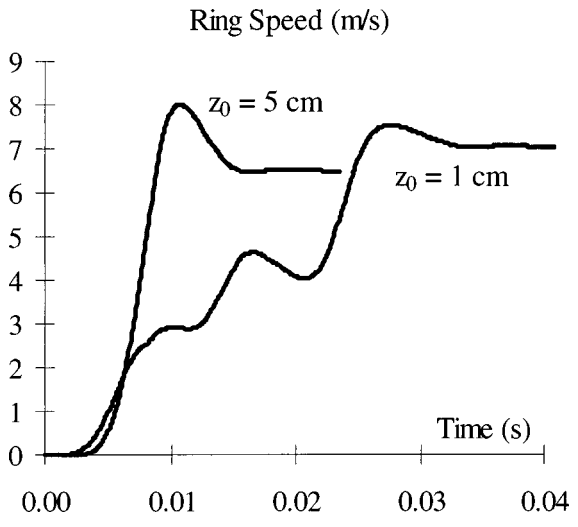

Fig. 15. Numerical integration of the force on the conducting ring gives its speed as a function of time, showing earlier repulsion when launched with greater height, z_0, above the center of the primary.

The time average over many cycles, assumed in the sinusoidal thin ring theory of the previous section, is valid in levitation and near the primary center. For most jumps, however, numerical integration is appropriate for accurate height calculation, and reversible permeability within the ring makes the jumping ring truly complex.

V. DEMONSTRATIONS

It is good to start demonstrations of the jumping ring with the 3.2-m vertical launch of a 1-in.-long Pasco aluminum ring. Jump heights for ring lengths of 6, 12, 25, and 50 mm exhibit a maximum at a small phase shift due to saturation of currents as mass increases, self-shielding of the primary's magnetic flux, and increasing average force for fast jumps. Nearly fourfold increases in conductivity at liquid nitrogen temperatures cause spectacular effects for small rings, double the 1-in. Pasco ring jump height to 6.4 m, and cause smaller increases in the jump heights of large rings as predicted in Eq. (14) and Fig. 9. The asymptotic jump height at high conductivity also applies to superconducting rings, while a slit ring with zero conductance does not jump. Similar results can be obtained with copper rings machined from bulk copper, but not from copper pipe, which is formed with a poorly conducting seam along its length. The joule of energy of a 50-mm-long Pasco ring, calculated from Eq. (10), can be demonstrated through the sound as it strikes a foot square thin brass plate balanced on one corner. Even the conductivity of an iron ring cut from a pipe and launched from a centimeter below the solenoid top will cause a diamagnetic jump of several centimeters before its ferromagnetism dominates.

Impedance can be demonstrated through the increase in primary current with applied voltage to decrease to the resistance as the core saturates at voltages large compared to V_N, such as line voltage applied without the rods in the pipe. The hollow iron pipe allows a test of magnetic permeability of various cores manifested by changes in the jump height. Insertion of a wooden dowel shows that its negligible magnetization does not change the jump height. Insertion of a solid aluminum rod shows a few percent eddy current shielding of the inner core by a conductor. Insertion of a bundle of coat hanger rods gives a fourfold increase in the jump height over the empty pipe by doubling the flux, as in Eq. (14). Similarly, the jump height increases quadratically with voltage up to magnetic saturation. An iron-free primary with the same flux as our design would require 30 times as many turns of copper wire and larger diameter to prevent overheating. Each time the switch is closed to launch a ring, students can hear the magnetostrictive hum of the iron core, evidence that it is near rotational saturation.

Resistive heating in the iron core arises from induced currents, and the rate of temperature increase is the power divided by the heat capacity, which is about three times the ideal gas constant per mole. The iron pipe would heat at 8 K/s but is slit lengthwise on one side to eliminate eddy currents, which also serves to prevent shielding of the inner core. The half mole of copper wire in the primary has a heat capacity of 12 J/K and increases in temperature at 25 K/s while the circuit is closed. The aluminum ring heats at 100 K/s, and increases in temperature by about 2 K per cycle. Rings launched from the center or held in place can become very hot, while rings in levitation above the pole carry little current and heat slowly. Hot rings have lower conductivity

and do not jump as high. With the apparatus turned horizontal and the ring placed at the center of the primary, there is no energy gradient or force. Since accelerations are about 200 times that of gravity, placement is very sensitive and rings will accelerate left or right depending upon small displacements from center, which demonstrates Lenz's law.

ACKNOWLEDGMENTS

We acknowledge the many contributions of L. L. Tankersley, the machining of Jeff Walbert, the PIXE impurity determination by Dave Moore, the assistance of Dave Rector, the interest of Donald J. Treacy, and the support and patience of Carole Schneider in this effort.

[1]David O. Woodbury, *Beloved Scientist* (McGraw–Hill, New York, 1944), p. 179.
[2]Richard M. Sutton, *Demonstration Experiments in Physics* (McGraw–Hill, New York, 1938), pp. 349–350.
[3]Richard P. Feynman, Robert B. Leighton, and Matthew Sands, *The Feynman Lectures on Physics* (Addison–Wesley, Reading, MA, 1964), Vol. II, Chap. 16-3.
[4]*Physics Demonstration Experiments*, edited by Harry F. Meiners (The Ronald Press, New York, 1970), Vol. II, pp. 945–948.
[5]S. Y. Mak and K. Young, ''Floating metal ring in an alternating magnetic field,'' Am. J. Phys. **54** (9), 808–811 (1986).
[6]*The Video Encyclopedia of Physics Demonstrations*, edited by Rosemary Wellner (The Education Group, Los Angeles, CA, 1992), Demonstration 20-18.
[7]Jonathon Hall, ''Forces on the Jumping Ring,'' Phys. Teach. **35**, 80–83 (1997).
[8]David J. Griffiths, *Introduction to Electrodynamics* (Prentice-Hall, Englewood Cliffs, NJ, 1981), Chaps. 2–7.
[9]Richard M. Bozorth, *Ferromagnetism* (Van Nostrand, New York, 1951), p. 846.
[10]Carl S. Schneider, Paula Y. Cannell, and Kimball T. Watts, ''Magnetoelasticity for Large Stresses,'' IEEE Trans. Magn. **28**, 2626–2631 (1992), see Eq. (7).
[11]Frederick W. Grover, *Inductance Calculations* (Van Nostrand, New York, 1946), pp. 143–147. Nagaoka's 1908 article is referenced and his computations are tabulated.
[12]William Fuller Brown, Jr., ''Domain Theory of Ferromagnetics Under Stress. III. The Reversible Susceptibility,'' Phys. Rev. **54**, 279–287 (1938).